13

A Flux Splitting Scheme with High-Resolution and Robustness for Discontinuities

Yasuhiro WADA
Computational Sciences Division, National Aerospace Laboratory in Tokyo, Japan
and
Meng-Sing LIOU
NASA Lewis Research Center in Cleveland, Ohio, U.S.A.

ABSTRACT

A flux splitting scheme is presented for the general non-equilibrium flow equations with an aim at removing numerical dissipation of Van-Leer-type flux-vector splittings on a contact discontinuity. The scheme is also recognized as an improved Advection Upwind Splitting Method(AUSM) where a slight numerical overshoot immediately behind the shock is eliminated. The proposed scheme has favorable properties: high-resolution for contact discontinuities; conservation of enthalpy for steady flows; numerical efficiency; applicability to chemically reacting flows. In fact, for a single contact discontinuity, even if it is moving, this scheme gives the numerical flux of the exact solution of the Riemann problem. Numerical experiments indicate no oscillation and robustness of the scheme for strong shock/expansion waves. Higher-order extension is also discussed.

1. INTRODUCTION

Recently various high-resolution schemes have been devised for the Euler/Navier-Stokes equations. Most of these schemes make use of a first-order upwind differencing as a basis, achieving higher-order accuracy under some restriction such as Total Variation Diminishing(TVD). Since these high-resolution schemes inherit their characteristics from their basic schemes, it is very important to design a basic scheme with desirable properties. Up to now, the basic upwind schemes have been proposed, and most of them are categorized as either Flux Difference Splitting(FDS) or Flux Vector Splitting(FVS): the former uses an approximate solution of the local Riemann problem, while the latter splits the flux vector into up-stream and down-stream traveling components. To our understanding, the most popular and successful FDS is Roe's scheme, while such a FVS is Van Leer's. However, neither of them are not a perfect flux splitting scheme: the former produces an expansion shock and fails near low density, while the latter bears large dissipation on contact discontinuities and shear layers. Generally speaking, the FDS schemes are too less dissipative and the FVS ones are too dissipative. There is an effort to design a robust FDS scheme, or a less dissipative FVS. However, the former scheme such as HLLEM[1] may be a little complicated scheme for practical application, and the latter effort was found to be a dead end[2].

There has been also a new approach to design a robust and less dissipative flux splitting scheme, in which the surplus dissipation of the FVS is reduced by introducing the flavor of FDS into FVS schemes. We call this approach FV/DS. Hänel[3] has found that the numerical dissipation in the boundary layer is greatly reduced by using one-sided upwinding of the tangential velocity in Van Leer's FVS formulation. This was later extended by Van Leer, who employed one-sided upwinding also for the enthalpy of the energy flux[4]. But both of these schemes still hold the numerical dissipation for 1-D contact discontinuities and yield glitches in the pressure near the edge of the boundary layer. Liou and Steffen proposed a more promising scheme named Advection Upstream Splitting Method(AUSM)[5, 6], in which the cell-face advection Mach number is appropriately defined to determine the upwind extrapolation for the convective quantities. The AUSM can capture a stationary contact discontinuity with no numerical dissipation and is robust enough to calculate strong shock waves. However, it bears a slight numerical overshoot immediately behind the shock.

In this paper, we present another way to remove the numerical dissipation of the Van-Leer-type flux-vector splittings on a contact discontinuity. Our basic idea is very simple: Van Leer's velocity splitting formula is modified so as to cancel the mass flux at the contact discontinuity. This scheme is also recognized as an improved AUSM scheme. A cure for the carbuncle phenomenon and higher-order extension are discussed as well.

2. GOVERNING EQUATIONS

2.1 Generalized Nonequilibrium Flow Equations

Generally, a nonequilibrium flow such as described by chemical reactions or turbulent models has the governing equations in a form:

$$\frac{\partial \mathbf{q}}{\partial t} + \frac{\partial \mathbf{F}_k}{\partial x_k} = \mathbf{S}, \tag{1}$$

where

$$\mathbf{q} = \begin{bmatrix} \rho \\ \rho u_1 \\ \rho u_2 \\ \rho u_3 \\ E \\ \rho f_1 \\ \rho f_2 \\ \vdots \\ \rho f_n \end{bmatrix}, \quad \mathbf{F}_k = \begin{bmatrix} \rho u_k \\ \rho u_1 u_k + \delta_{1,k} p \\ \rho u_2 u_k + \delta_{2,k} p \\ \rho u_3 u_k + \delta_{3,k} p \\ (E+p) u_k \\ \rho f_1 u_k \\ \rho f_2 u_k \\ \vdots \\ \rho f_n u_k \end{bmatrix}, \quad \mathbf{S} = \begin{bmatrix} 0 \\ 0 \\ 0 \\ 0 \\ 0 \\ s_1 \\ s_2 \\ \vdots \\ s_n \end{bmatrix},$$

$$E = e + \frac{1}{2}\rho({u_1}^2 + {u_2}^2 + {u_3}^3),$$

and

$$p = p(\rho, e, \rho f_1, \rho f_2, \ldots, \rho f_n). \quad (2)$$

These equations include the conservation of total mass, momentum, total energy, and also the physical quantities ρf_i, which represent nonequilibrium effects, *i.e.*, either the concentration of chemical species or vibrational energy. The quantities p, ρ, u_k, E, and e respectively denote the pressure, density, Cartesian velocity components, total and internal energies, whereas the vector **S** is a set of elements of nonequilibrium source terms. It is assumed that an appropriate "*frozen*" speed of sound c is calculated depending on a gas model, by which Eq.(2) is defined. In this study, a numerical scheme is formulated for the governing equations given by Eqs.(1) and Eq.(2).

2.3 Numerical Flux in Generalized Coordinates

In practical computation, a numerical flux in generalized coordinates is needed, which we calculate after [7]. Let the vector $\mathbf{n} = (n_1, n_2, n_3)$ be a normalized cell-interface normal in ξ-direction with the vectors $\mathbf{l}(l_1, l_2, l_3)$ and $\mathbf{m}(m_1, m_2, m_3)$ being its recipropal ones: $\mathbf{n}\cdot\mathbf{l} = 0$; $\mathbf{n}\cdot\mathbf{m} = 0$; $\mathbf{l}\cdot\mathbf{m} = 0$; $|\mathbf{n}| = |\mathbf{l}| = |\mathbf{m}| = 1$. The normal and tangential velocity components to the cell-interface normal are calculated for each left and right state:

$$u = n_i u_i, \quad v = l_i u_i, \quad w = m_i u_i. \quad (3)$$

The numerical flux in the x-direction of this local Cartesian coordinates has the form:

$$\mathbf{F} = (\rho u, \rho u^2 + p, \rho v u, \rho w u, \rho H u, \rho f_1 u, \ldots \rho f_n u)^t \quad (4)$$

where H is the total enthalpy:$H \equiv (E + p)/\rho$. Following a specified flux splitting scheme, the numerical flux $\mathbf{F}_{1/2} = (F_1, F_2, \ldots, F_{5+n})^t$ is calculated in these local Cartesian coordinates. Finally the numerical flux in the ξ-direction of the generalized coordinates, $\mathbf{F}_\xi$, is given as

$$\mathbf{F}_\xi = S \begin{bmatrix} F_1 \\ n_1F_2 + l_1F_3 + m_1F_4 \\ n_2F_2 + l_2F_3 + m_2F_4 \\ n_3F_2 + l_3F_3 + m_3F_4 \\ F_5 \\ F_6 \\ \vdots \\ F_{5+n} \end{bmatrix}, \quad (5)$$

where S is the area of the cell interface. In this procedure the numerical flux in the generalized coordinates is uniquely specified by the definition of the numerical flux in the local Cartesian coordinates, which is discussed in the next section.

3. NUMERICAL SCHEME

3.1 Classification of the FV/DS schemes

Up to now, the most successful FV/DS schemes have been the Van Leer scheme[4] and the AUSM[5, 6]. These schemes are equipped with favorable properties: conservation of enthalpy for steady flows; small dissipation in the shear layer. As the first step in constructing our scheme, we generalize these schemes, calling them AUSMV-type and AUSMD-type schemes, where "V" and "D" denote flux-Vector-splitting-biased schemes and flux-Difference-splitting-biased ones, respectively.

First, we define the AUSMD-type schemes by its numerical flux:

$$\mathbf{F}_{1/2} = \frac{1}{2}[\,(\rho u)_{1/2}(\Psi_L + \Psi_R) - |(\rho u)_{1/2}|(\Psi_R - \Psi_L)\,] + \mathbf{p}_{1/2}, \quad (6)$$

where

$$\Psi = (1, u, v, w, H, f_1, \ldots, f_n)^t.$$

Hence, a specific numerical scheme is uniquely defined by an appropriate interface mass flux $(\rho u)_{1/2}$ and interface pressure $p_{1/2}$. So far, the interface pressure of Van Leer's FVS is usually used as $p_{1/2}$. On the other hand, the form of the mass flux varies with each numerical scheme, because the mass flux is directly connected to the resolution of contact discontinuities, which is a main interest in the FV/DS schemes. For example, the following mass fluxes may be possible for the AUSMD-type scheme, and are actually used in Van Leer's FV/DS and the AUSMs, respectively.

- Van Leer's FV/DS:
$$(\rho u)_{1/2} = u_L^+ \rho_L + u_R^- \rho_R. \quad (7)$$
- AUSM(velocity-splitting):
$$(\rho u)_{1/2} = \frac{1}{2}[\,u_{1/2}(\rho_L + \rho_R) - |u_{1/2}|(\rho_R - \rho_L)\,], \quad (8)$$
where $u_{1/2} = u_L^+ + u_R^-$.
- AUSM(Mach number-splitting):
$$(\rho u)_{1/2} = \frac{1}{2}[\,M_{1/2}(\rho_L c_L + \rho_R c_R) - |M_{1/2}|(\rho_R c_R - \rho_L c_L)\,], \quad (9)$$
where $M_{1/2} = u_L^+/c_L + u_R^-/c_R$.

Here $u^\pm$ are identical to the velocity splitting of Van Leer's FVS. The AUSM belongs to the AUSMD-type schemes. In fact, the interface mass flux defined by Eq.(8) or Eq.(9) in conjunction with the interface pressure of Van Leer's FVS makes the AUSMD-type scheme reduce to the velocity-splitting-based AUSM and the Mach-number-splitting-based AUSM, respectively. It is noted that the mass flux of the Mach-number-splitting-based AUSM vanishes at a stationary discontinuity, making the AUSM a less dissipative scheme among the FV/DS schemes. In the next section, we will present a new formula for the interface mass flux $(\rho u)_{1/2}$ which results in noticeable improvements over the AUSM.

The numerical flux of the Van Leer FV/DS scheme[4] slightly differs from the form of Eq.(6) even if the mass flux of Eq.(7) is used, because that scheme does not use the upwind extrapolation about the term $(\rho u^2)_{1/2}$ in the x-momentum flux. Hence, we need to define another class of FV/DS schemes — AUSMV-type schemes:

$$(\rho u^2)_{\mathrm{AUSMV}} = u_L^+ (\rho u)_L + u_R^- (\rho u)_R. \quad (10)$$

But the AUSMD-type schemes defines

$$(\rho u^2)_{\mathrm{AUSMD}} = \frac{1}{2}[\,(\rho u)_{1/2}(u_L + u_R) - |(\rho u)_{1/2}|(u_R - u_L)\,]. \quad (11)$$

The mass flux of Eq.(7) and the velocity/pressure splittings of Van Leer's FVS make the AUSMV-type scheme reduce to the Van Leer FV/DS scheme. We emphasize that a specific AUSMV-type scheme needs the definition of the velocity splitting, $u^{\pm}$, for the x-momentum flux as well as that of the interface mass flux and the pressure.

3.2 AUSMD and AUSMV Scheme

The main drawback of Van Leer's FV/DS scheme is the numerical viscosity on the contact surface, while that of the AUSM is the numerical overshoot at shock waves. We have found that the overshoot of the AUSM is mainly due to the mass flux differencing. This is probably because the AUSM mass flux of Eq.(8) nor Eq.(9) does not directly take into account of the density behind the shock wave. Hence, in this study we employ a mass flux formula of Eq.(7). In this case, however, the surplus numerical dissipation at the contact discontinuities is a problem.

In this study, we design a velocity splitting so that the numerical dissipation can cancel at the contact discontinuity. The mass flux is

$$(\rho u)_{1/2} = u_L^+ \rho_L + u_R^- \rho_R, \qquad (12)$$

where the velocity splittings u_L^+, u_R^- are no longer the familiar Van Leer splittings, but rather including terms designed to capture stationary/moving contact discontinuities, and are given as

$u_L^+ =$

$$\begin{cases} \alpha_L\{ \frac{(u_L+c_m)^2}{4c_m} - \frac{u_L+|u_L|}{2}\} + \frac{u_L+|u_L|}{2}, & \text{if } \frac{|u_L|}{c_m} \le 1; \\ \frac{u_L+|u_L|}{2}, & \text{otherwise,} \end{cases}$$

$u_R^- =$

$$\begin{cases} \alpha_R\{-\frac{(u_R-c_m)^2}{4c_m} - \frac{u_R-|u_R|}{2}\} + \frac{u_R-|u_R|}{2}, & \text{if } \frac{|u_R|}{c_m} \le 1; \\ \frac{u_R-|u_R|}{2}, & \text{otherwise,} \end{cases}$$

where

$$\alpha_L = \frac{2\,(p/\rho)_L}{(p/\rho)_L + (p/\rho)_R}, \quad \alpha_R = \frac{2\,(p/\rho)_R}{(p/\rho)_L + (p/\rho)_R},$$

and $c_m = \max(c_L, c_R)$. The velocity splitting, which is a function of α: $0 \le \alpha \le 2$, is shown in Fig. 1.

Secondly, the pressure flux is

$$p_{1/2} = p_L^+ + p_R^-, \qquad (13)$$

where

$$p_{L/R}^{\pm} = \begin{cases} p_{L/R}(\frac{u_{L/R}}{c_m} \pm 1)^2(2 \mp \frac{u_{L/R}}{c_m})/4, & \text{if } \frac{|u_{L/R}|}{c_m} \le 1; \\ p_{L/R}\frac{u_{L/R} \pm |u_{L/R}|}{2\,u_{L/R}}, & \text{otherwise.} \end{cases}$$

Substitution of Eq.(12) and Eq.(13) into Eq.(6) results in the numerical flux of the AUSMD, in addition, if the term ρu^2 in the x-momentum flux is replaced by Eq.(10), we have the scheme AUSMV. We call these specific AUSMD/V-type schemes as the AUSMD and AUSMV, respectively.

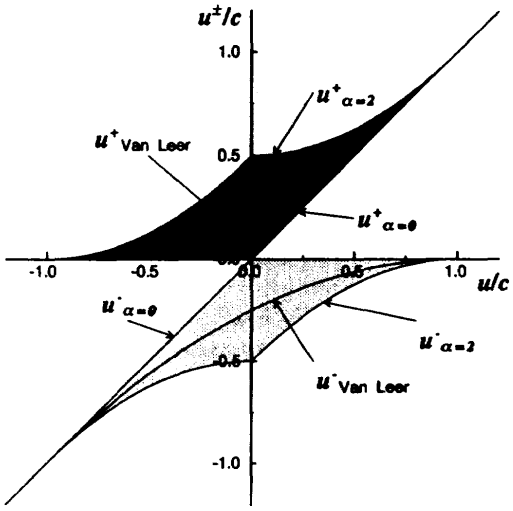

Fig. 1 Velocity splitting.

3.3 AUSMDV: Mixture of AUSMD and AUSMV

There remains a question about the choice between the AUSMD and AUSMV, *i.e.*, between Eq.(11) and Eq.(10). According to our numerical experiments[8], the AUSMV has a higher shock-capturing capability than the AUSMD, while the AUSMD has a weaker CFL number restriction than the AUSMV. Then we prefer a mixed momentum flux of $(\rho u)_{1/2}$ between the AUSMV and AUSMD:

$$(\rho u^2)_{1/2} = (\frac{1}{2}+s)(\rho u^2)_{\text{AUSMV}} + (\frac{1}{2}-s)(\rho u^2)_{\text{AUSMD}}, \qquad (14)$$

where s is a switching function of the pressure gradient:

$$s = \frac{1}{2}\min(1,\, K\frac{|p_R - p_L|}{\min(p_L, p_R)}) \qquad (15)$$

This averaging is biased toward to the AUSMV in order to maintain the shock-capturing capability. We call this mixed scheme the AUSMDV. In this study a constant parameter $K = 10$ is taken. It is noted here that the genuine AUSMV flux is also possible when the CFL restriction is not considered serious.

3.4 A Cure for the Carbuncle Phenomenon

The carbuncle phenomenon is an instability in capturing a strong shock wave in multi-dimensional problems. Quirk's proposed a test problem[9], in which a shock wave propagates into a static gas through a duct whose centerline grid is slightly perturbed. The AUSMDV is not free from this problem as shown in Fig. 2. We suspect that the carbuncle phenomenon comes from the recognition of a multi-dimensional shock wave by a one-dimensional numerical scheme. When the shock wave is captured by a shock capturing scheme, an intermediate point(s), which is unphysical, is needed to express a shock position numerically. In 1-D case, if the scheme is well designed, this is not a problem. But when that scheme is applied to multi-dimensional calculation, the intermediate point exchanges information with the neighbors which are also intermediate shock points. It is probable that the exchange of information between these unphysical data causes a numerical instability. In that case, a mechanism to stabilize the shock or some form

of artificial viscosity is required. We call this artificial procedure "*Shock-Fix*."

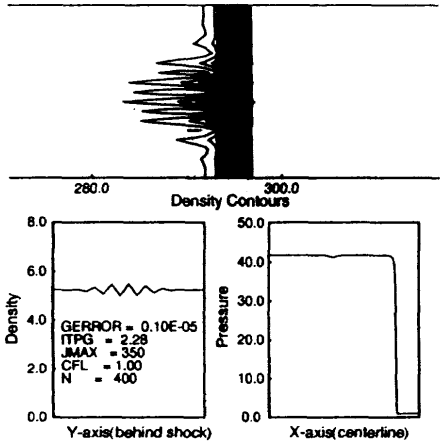

Fig. 2 Shock wave propagating through a duct by AUSMDV.

Here, the following shock-fix is proposed(see Fig.3).

1. Find out compressible sonic points across the cell interface before calculating numerical flux. This sonic point takes place when

$$\begin{cases} u_L - c_L > 0 \text{ and } u_R - c_R < 0, \\ \text{or } u_L + c_L > 0 \text{ and } u_R + c_R < 0. \end{cases} \quad (16)$$

   If this is detected between grid point j and $j+1$, set flag $S_{\xi,j} = 1$ and $S_{\xi,j+1} = 1$ in ξ-direction. The same procedure is done in η/ζ-direction, which is easy to vectorize.

2. In calculating a numerical flux in ξ-direction between grid points j and $j+1$, S_η and S_ζ but S_ξ are used to sense the shock position, to which some dissipative scheme is applied. That is

$$\begin{cases} \text{Dissipative Scheme: if} \\ \quad (S_{\eta,j} + S_{\eta,j+1} + S_{\zeta,j} + S_{\zeta,j+1}) \geq 1; \\ \text{Non-Dissipative Scheme: otherwise.} \end{cases}$$

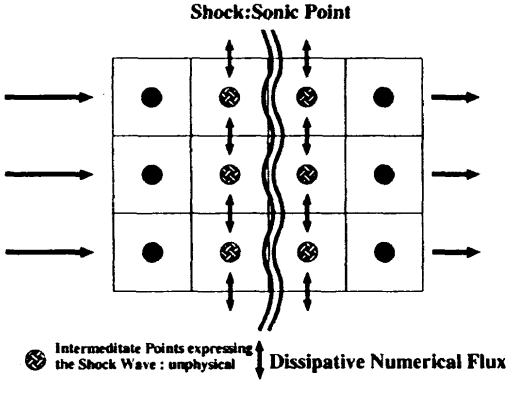

Fig. 3 Shock-fix.

The numerical fluxes in other directions are calculated in a similar way. This method unlike [9] does not use the pressure gradient in sensing shock waves. The pressure gradient does not always provide a sufficient information for the recognition of shock wave, since in that case some empirical parameter to distinguish shock and compressive wave would be needed. It is noted that the alone shock fix procedure is easily applicable to unstructured grid approach. This shock-fix needs a dissipative scheme to stabilize the shock wave. For the AUSMDV, we employ Hänel's FVS scheme, because it is dissipative enough and conserves the total enthalpy for steady flows. The numerical flux of Hänel's FVS is

$$\mathbf{F}_{1/2} = \rho_L u_L^+ \Psi_L + \rho_R u_R^- \Psi_R + \mathbf{p}_{1/2}, \quad (17)$$

where the velocity splitting and the interface pressure are identical to those of Van Leer's FVS. Quirk[9] proposed a test problem for the carbuncle phenomenon, where a shock wave propagates into a static gas through a duct whose centerline grid is slightly perturbed. Figure 4 show the solution of Quirk's test problem by the AUSMDV without the shock-fix, indicating the effectiveness of the shock-fix. A similar shock-fix is possible for Roe's approximate Riemann solver, for which the HLLE scheme is considered to be a dissipative partner scheme[8].

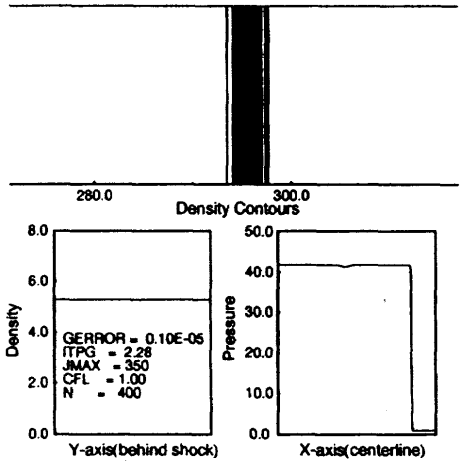

Fig. 4 Shock wave propagating through a duct by AUSMDV with shock-fix.

4. RESULTS AND DISCUSSIONS

4.1 Test Problems using First-Order Scheme

Here some of numerical experiments are introduced. The first problems are shock-tube ones as shown in Fig. 5a-c, where the initial value is

- $(\rho, p, u)_L = (1, 1, 0); (\rho, p, u)_R = (1/8, 1/10, 0)$,
- $(\rho, p, M)_L = (.1, .1, 15); (\rho, p, M)_R = (.1, .1, -15)$,
- $(\rho, p, u)_L = (1, 2, -2.5c_L); (\rho, p, u)_R = (1, .5, 2.5c_L)$,

respectively. The first case is Sod's standard problem and the other problems are about very strong shock and expansion waves. All these figures indicate the robustness and high-resolution of the AUSMDV. The second problem is 1-D self-similar conical flow over a 10-degree half cone at hypersonic speed. This problem is used to check the accuracy of numerical schemes on the shock and boundary layer[10]. The flow conditions are $M_\infty = 7.95; Re_\infty = 4.2\times10^5$. Figure 6 shows the profiles of pressure, temperature and tangential velocity solved by the AUSMDV. The AUSMDV conserves the total enthalpy for a steady state solution, giving the exact wall temperature solution indicated by an arrow. In addition, the thickness of the boundary layer was very similar to that solved by the Roe scheme, indicating high-resolution of the AUSMDV for a non-linear wave discontinuity as well. Other various numerical experiments including thermo-chemical non-equilibrium flows are found in [8].

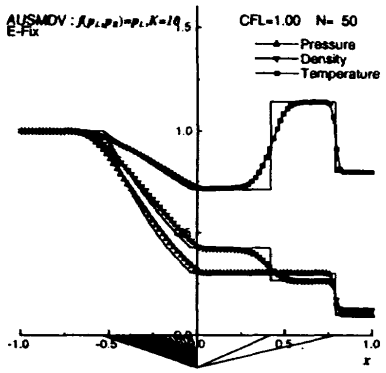

Fig. 5a Sod's shock-tube problem.

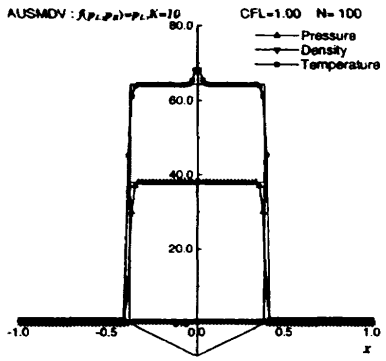

Fig. 5b Shock-tube problem — colliding flow.

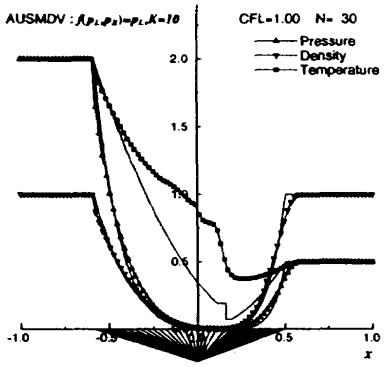

Fig. 5c Shock-tube problem — strong expansion.

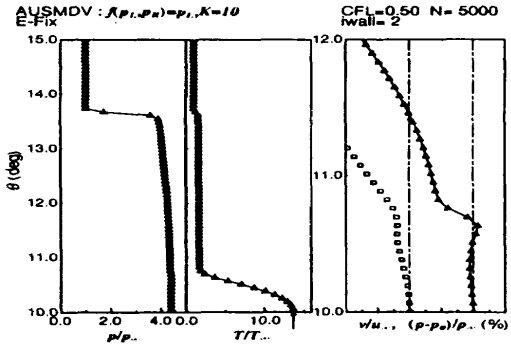

Fig. 6 Conical flow problem.

4.2 MUSCL Higher-Order Extension

I is natural to use the MUSCL approach in extending the AUSMDV to higher-order accuracy. However, there are arbitrariness for the choice of variables which are interpolated or extrapolated. We may choose conservative variables $\mathbf{q} = (\rho, \rho u, E)$, or primitive variables $\hat{\mathbf{q}} = (\rho, u, p)$. Even when the characteristic decomposition is used, there are still many choices about which kind of governing equations is used in deriving the characteristic variables. For example, the governing equations for the conservative variables $\mathbf{q}$ give $\mathbf{L}\Delta\mathbf{q}$ as gradient of characteristics, while those for the primitive ones do $\hat{\mathbf{L}}\Delta\hat{\mathbf{q}}$, where $\mathbf{L}$ and $\hat{\mathbf{L}}$ are left-eigenvector matrix for the conservative variables and primitive ones, respectively. Here, in order to show the effects of choice of the variables extrapolated, some numerical results are presented. Figures 7a and 7b show the solution for Sod's shock-tube problem using the primitive variables $\hat{\mathbf{q}} = (\rho, u, p)$ and the characteristic variables based on $\hat{\mathbf{q}}$. Here the minimod was used as a limiter function. The MUSCL approach using the characteristic variables gives obviously better solution than the non-characteristic ones. This tendency was common for other sets of variables, $(\rho, \rho u, E), (\rho, u, T), (T, u, p)$ and (H, u, p), with the difference among the results using characteristics variables being very minor, although they are not shown in this paper.

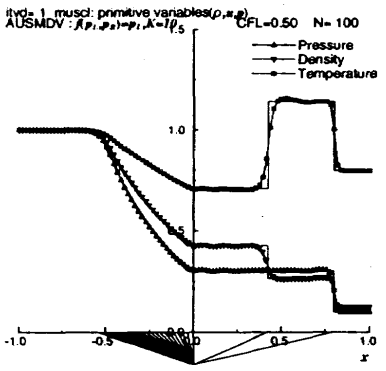

Fig. 7a Sod's shock-tube problem — MUSCL $\Delta(\rho, u, p)$

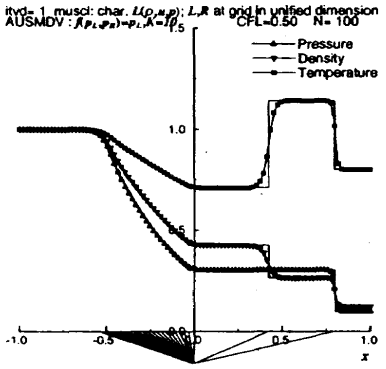

Fig. 7b Sod's shock-tube problem — MUSCL $\mathbf{L}\Delta(\rho, u, p)$

Secondly the conical flow problem is solved by the AUSMDV with the MUSCL higher-order extension. Figures 8a-e present the results. For this steady state problem, the characteristic decomposition shows almost no improvements over the use of raw variables. Within the boundary layer the pressure is constant, but temperature and density have a steep gradient. Then, the reconstruction using the temperature and density can not recover the physically correct pressure profile as shown in Figs. 8c and 8d. On the other hand, when the pressure is included as a element of extrapolated variables, a fairly good result is obtained as shown in Fig. 8a, 8b and 8e. The solution in Fig. 8e uses the characteristic variables in which the total enthalpy H is included as a extrapolated variable, keeping the conservation of H for

a steady state solution even at higher-order accuracy. Also the use of variables (T, u, p) gives a good solution similar to that by using (H, u, p), being advantageous for chemically reacting flow problems because of no need of calculating temperature by the Newton iteration. It is noted here that there were almost no difference between the Roe scheme and the AUSMDV as a basic flux splitting scheme in the above calculations. More detailed study about the choice of variables used in the MUSCL approach will be reported in near future[11].

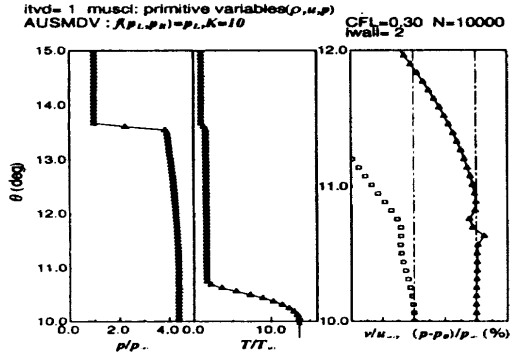

Fig. 8a Conical flow problem — MUSCL $\Delta(\rho, u, p)$

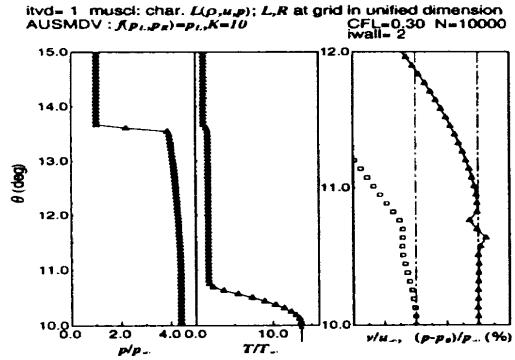

Fig. 8b Conical flow problem — MUSCL $L\Delta(\rho, u, p)$

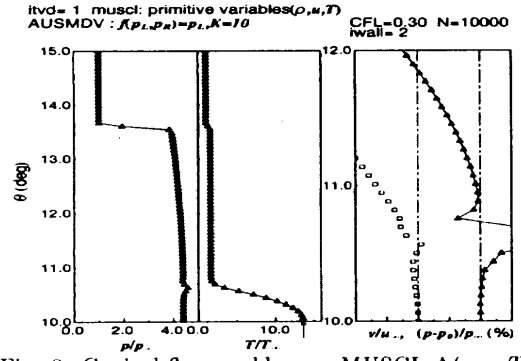

Fig. 8c Conical flow problem — MUSCL $\Delta(\rho, u, T)$

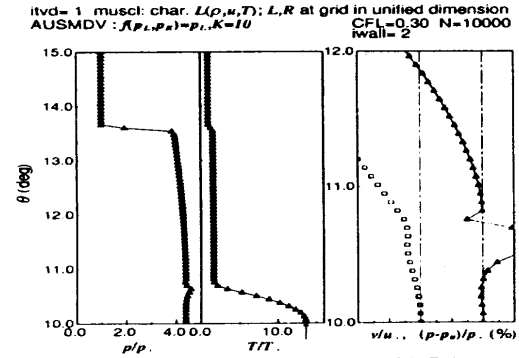

Fig. 8d Conical flow problem — MUSCL $L\Delta(\rho, u, T)$

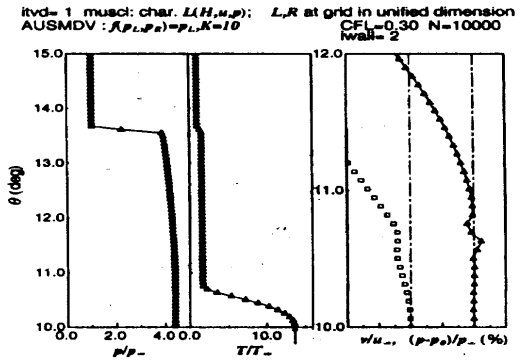

Fig. 8e Conical flow problem — MUSCL $L\Delta(H, u, p)$

5. CONCLUSION

We have presented a flux splitting scheme equipped with favorable properties: high-resolution for contact discontinuities; conservation of enthalpy for steady flows; numerical efficiency; applicability to chemically reacting flows. Numerical experiments indicate the soundness of the proposed scheme. Higher-order extension is also discussed.

ACKNOWLEDGMENT

This work was partly done while the first author stayed at NASA Lewis Research Center.

REFERENCES

[1] Wada, Y., "On the Godunov-Type Schemes — An Improvement of HLLEM Scheme and its Extension to Chemically Reacting Flows," NAL TR-1189, 1993.

[2] Coirier,W.,J. and Van Leer, B., "Numrical Flux Formulas for the Euler and Navier-Stokes Equations: II. Progress in Flux-Vector Splitting," AIAA Paper 91-1566CP, 1991.

[3] Hänel, D. and Schwane, R., "An Implicit Flux-Vector Splitting Scheme for the Computation of Viscous Hypersonic Flow," AIAA Paper 89-0274, January 1989.

[4] Van Leer, B., "Flux-Vector Splitting for the 1990s," NASA CP-3078, 1991, pp.203-214.

[5] Liou, M.-S. and Steffen,C.J., "A New Flux Splitting Scheme," NASA TM104404, 1991; also in *J. Comput. Phys.* vol.107, 1993, pp. 23-39.

[6] Liou, M.-S., "On a New Class of Flux Splittings," Lecture Notes in Physics, vol.414, 1993, pp.115-119.

[7] Anderson, W.K., Thomas, J.L. and Van Leer, B., "Comparison of Finite Volume Flux Vector Splittings for the Euler Equations," *AIAA Journal*, vol.24, 1986, pp.1453-1460; also AIAA Paper 85-0122, January 1985.

[8] Wada, Y. and M.-S. Liou, "A Flux Splitting Scheme with High-Resolution and Robustness for Discontinuities," AIAA Paper 94-0083, January 1994.

[9] Quirk, J.J., "A contribution to the Great Riemann Solver Debate," ICASE Report 92-64, 1992.

[10] Van Leer, B., Thomas, J.L., Roe, P.L., Newsome, R.W., "A Comparison of Numerical Flux Formulas for the Euler and Navier-Stokes Equations," AIAA Paper 87-1104CP, 1987.

[11] Wada, Y. and Liou,M.-S., in preparation.